Appl. Phys. B 66, 741–745 (1998)

Applied Physics B
Lasers
and Optics

Photoacoustic trace-gas detection using a cw single-frequency parametric oscillator

F. Kühnemann[1,*], K. Schneider[2,], A. Hecker[1], A.A.E. Martis[1], W. Urban[1], S. Schiller[2], J. Mlynek[2]**

[1] Institut für Angewandte Physik der Universität Bonn, Wegelerstraße 8, D-53115 Bonn, Germany
[2] Universität Konstanz, Fakultät für Physik, Postfach 5560-M696, D-78457 Konstanz, Germany

Received: 28 January 1998/Revised version: 9 April 1998

Abstract. We report extra-cavity photoacoustic trace-gas detection of ethane (C_2H_6) at 3.34 μm using a widely tunable cw single-frequency optical parametric oscillator. The high frequency and power stability and the continuous tunability of the parametric oscillator make it ideally suited for this application. Detection sensitivities of 0.5 ppb for ethane are obtained, which is comparable to the best results previously obtained with intracavity detection using line-tunable CO overtone lasers. The flexibility and compact size of cw single-frequency parametric oscillators can lead to portable photoacoustic trace-gas detection systems for environmental monitoring and process control.

PACS: 42.65; 82.80K

Infrared spectroscopic methods are known to be very sensitive tools for trace-gas detection. The infrared fingerprint spectra of the molecules allow the detection of these gases in concentrations at the ppb level and below. For this, absorption coefficients of $\alpha = 10^{-9}\,\mathrm{cm}^{-1}$ have to be detected. Besides absorption techniques, which usually use long paths (up to a kilometer in multi-pass cells), photoacoustic spectroscopy (PAS) has proven to be a very powerful technique [1–3]. The amount of infrared radiation, absorbed by the molecules, is measured indirectly through its subsequent conversion into heat. When the exciting laser beam is interrupted (chopped) at an acoustic frequency, this results in the formation of an acoustic wave with an amplitude proportional to the concentration. Operation at a resonance frequency of the cell ('resonant PA cell') increases the sensitivity. Since the magnitude of the PA signal scales with the incident infrared power, laser power greater than 100 mW is required for high-sensitivity detection. That is why up to now mainly gas lasers are used as photoacoustic laser sources. The CO_2 laser [4–6] (9–11 μm), the CO laser [7] (4.8–8.4 μm), and the CO-overtone laser (2.8–4.1 μm) [8–10] together cover a considerable fraction of the infrared fingerprint region and allow the detection of a large number of environmentally or biologically relevant gases [3]. If the PA cell is placed in the laser cavity, power levels up to 140 W with the CO_2 laser [5], 25 W with the CO laser [9], and 5 W with the CO overtone laser [10] are available for photoacoustic detection. As an example, with the CO_2 laser system ethylene concentrations of some 10 ppt can be detected corresponding to absorption coefficients of about $10^{-10}\,\mathrm{cm}^{-1}$ in a cell volume of only 10 cm^3 [5, 6]. This sensitivity makes PAS a powerful tool, for example in plant physiological studies, where the available sample volume is limited and time resolution is an issue. Very low emission rates of volatile organic compounds such as ethylene, ethane, and acetaldehyde can deliver important information on the metabolic state of plants or fruits [11], and PAS has demonstrated its great potential in this field in a number of applications (e.g. [12, 13]). Ethane, an indicator of plant cell damage, can now be detected down to about 140 ppt by using the CO overtone laser PA spectroscopy [10].

The CO and CO overtone lasers operate, however, on discrete laser lines with separations $\geq 1\,\mathrm{cm}^{-1}$. Thus the detection of a given molecule depends on accidental coincidences between the laser lines and the absorption features of the molecules. The PA detection at atmospheric pressure not only ensures an effective vibrational–translational relaxation but also improves to some extent the chances for accidental coincidences due to the collisional broadening of the absorption lines to between 0.1 and 0.5 cm^{-1}. Selectivity of the trace-gas detection, however, is reduced in comparison with Doppler-broadened spectra due to the spectral overlap of the absorption features of different gases.

These facts strongly motivate the search for new radiation sources that allow the free selection of any desired wavelength within a broad spectral range together with a continuous tuning over a range on the order of a pressure broadened linewidth (several GHz). Moreover, these sources should provide a power level comparable to the gas lasers. With such a source the strongest absorption features of a given trace gas could be used for the detection without the limitation of accidental coincidences. This in turn would allow systematic studies of detection at reduced pressure with the chance of improved selectivity. In addition, the development of more compact and efficient broadly tunable light sources that fulfill the requirements for PA detection are highly desirable for mobile trace-gas detection systems.

* Fax: +49-228/733-474, E-mail: kuehne@iap.uni-bonn.de
** deceased

In the last few years several new sources based on solid-state systems have been developed. Difference-frequency generation (in part pumped by tunable diode lasers) now delivers radiation up to 15 μm [14] and compact solid-state systems have been applied to trace gas detection. A few μW of infrared power are sufficient for long-path absorption measurements, as has been demonstrated with methane detection around 3.4 μm with ppb level accuracy [15]. Such power levels are, however, too low for sensitive photoacoustic detection. Tunable diode lasers in the near infrared (0.8–1.6 μm) allow trace-gas detection using overtones of molecular vibrations [16], but the advantage of higher power and simple operation cannot compensate the small transition dipole moments of the overtone vibrations, which result in comparatively poor detection limits.

Pulsed narrow-band optical parametric oscillators have been used for PA spectroscopic demonstrations in the near infrared [17], and, in combination with difference-frequency generation, also in the mid-infrared [18]. Studies with pulsed CO_2 laser PA systems [19] applied for C_2H_4 detection have shown, however, that the sensitivity of pulsed systems remains inferior to cw resonant systems.

In contrast to that, completely new opportunities arise from the development of cw OPO systems that fulfill the following requirements: single-frequency emission over a broad spectral range, mode-hop-free operation with high frequency stability (better than 100 MHz) over typical measurement times, free selection of any frequency within the emission range, and sufficiently high power (> 100 mW). In principle, both doubly resonant [20, 21] and singly resonant OPO [22–24] configurations could be used for this purpose. However, the single-frequency SRO with its demonstrated capability of a broad tuning range [25] makes it the candidate of choice. The development of quasi-phasematched materials, such as periodically poled lithium niobate [26], has lead to cw OPOs with output powers at the watt level in the 3–4-μm range with multimode output [27]. The operation of a cw singly resonant OPO with single-frequency output, as well as high frequency and power stability, as is required for PA and most other spectroscopy techniques, has been demonstrated recently [25].

The purpose of the present paper is to demonstrate the applicability of the cw parametric oscillator for photoacoustic trace-gas detection and to determine the present detection limit. For this purpose the new cw OPO [25] was combined with a photoacoustic system as used for high sensitivity detection of C_2H_4 using a CO_2 laser [6]. Ethane (C_2H_6) was chosen as the model gas, since it is important in plant physiological studies [11] and its spectrum in the 3–4-μm range is well suited to demonstrate the advantages of the pump source.

1 Experimental setup

A schematic of the experimental setup is shown in Fig. 1. Our tunable laser source is a singly resonant optical parametric oscillator (SRO) pumped by a 1064-nm single-frequency laser [25]. The pump wave is resonated in the SRO cavity in order to reduce the threshold to an accessible level. The SRO delivers radiation at almost any frequency in the spectral range of 1.45–2 (signal) and 2.3–4 μm (idler) with output powers at the 100-mW level in the idler branch. The broad spectral coverage is achieved by using a so-called "multi-grating" lithium niobate crystal on which several sections of different periodicity were patterned. Coarse tuning of the output wavelengths is achieved by selection of a particular quasi-phasematching grating. Finer tuning is obtained by changing the crystal temperature. Finally, tuning of the pump laser frequency allows tuning with the highest resolution, the continuous tuning range being a few GHz. The frequency instability of the parametrically generated waves is below 30 MHz/h with linewidths better than 5 MHz. The minimum external threshold is 135 mW at 2.4 μm and a maximum total conversion efficiency of 30% is achieved at a pump power of 780 mW. The SRO reliably operates over many hours with power fluctuations less than 1% and without mode hops thanks to the frequency stability of the pump laser and the chosen SRO configuration, in which the OPO cavity length is stable because it is servo-controlled to resonate the pump wave. Since the pump source is a miniature Nd:YAG ring laser and the semimonolithic SRO cavity is 3 cm long, the complete system is rather compact. The parametrically generated light is extracted with a dichroic mirror. The signal wave is separated from the idler wave with another dichroic mirror and injected into a wavemeter to monitor its wavelength. From its value, the corresponding idler wavelength could be inferred after calibration of the pump wavelength.

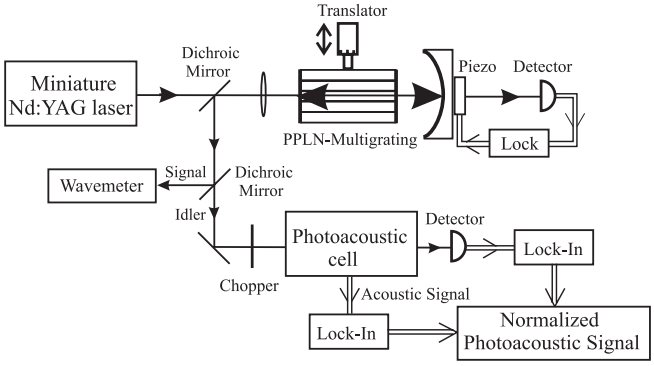

Fig. 1. Scheme of the experimental setup

The photoacoustic cell is of the resonant type operated at its first longitudinal mode at about 2 kHz. The resonator is a stainless steel tube with a length of 80 mm and an inner diameter of 14 mm. An electret microphone (Knowles EK3027) is mounted flush into the wall at the anti-node of the acoustic wave. The resonator tube is placed in a massive aluminum body (the PA cell) for acoustic shielding against lab noise. For further acoustic shielding the complete cell is placed in a massive fiber board box, coated with foam on the inside.

The laser beam enters and leaves the cell through ZnSe windows mounted at the Brewster angle to avoid back reflections into the cell. Large buffer volumes with a diameter of 10 cm and a lengths of 4 cm ($= \lambda/4$) act as acoustic filters between the windows and the resonator and isolate the latter from coherent background signals originating from the windows or molecular layers adsorbed on the windows.

The beam is focused into the PA cell with a waist of approximately 0.5 mm by using a gold-coated mirror with roc = 1 m. At the Brewster windows the beam radius was about 1.5 mm. Due to the sufficiently large diameter of the resonator (14 mm) no special care has been necessary during the alignment to avoid wall signals. After exiting the PA

cell the idler wave is focused onto a pyroelectric detector for power monitoring. Average power levels of 40 mW (unchopped) were measured behind the PA cell. To generate a PA signal the beam is chopped by a phase-locked chopper. Microphone and detector signals (amplitude and phase) are both processed with two-channel lock-in amplifiers and recorded with a 10-s time constant.

The chopper frequency is controlled by the internal reference of the microphone lock-in amplifier. Its stability of < 1 Hz at 2 kHz is sufficient to match the resonance of the PA cell, which has a halfwidth of about 25 Hz. In the air-conditioned lab the temperature is stable within 1 °C, which results in a maximum drift of the resonance frequency of about 4 Hz within 24 h. Thus all drifts in resonance frequency could be corrected manually.

The gas flow (up to 2 l/h) is injected into the resonator through a central inlet (0.8 mm diameter), and the gas leaves the cell through the buffer volumes. Thus a fast exchange of the air in the resonator is ensured which allows us to detect changes in trace-gas concentration as fast as a minute. A commercially available mixture of ethane (0.98 ppm) in nitrogen (99.999%) has been used for the PA measurements. To determine the background signal (i.e. no absorbing gas present) the cell is flushed with nitrogen (99.999%). The N_2 is additionally purified by using a LN_2 cooling trap. For ultimate purity of the PA cell a flushing for 24 hours or longer is necessary to remove any possible impurities. Gas flow is maintained and monitored with two flow controllers and the pressure in the cell is monitored with a capacitance manometer.

2 Results

One of the aims of the OPO application is to improve the sensitivity of the trace gas detection by using the strongest absorption features available in the respective wavelength range which becomes possible with the OPO. In the range of the CO overtone laser ethane (C_2H_6) shows a very strong absorption due to the degenerate ν_7 ro-vibrational band, centered at 2985.4 cm^{-1}. The central part of the band is shown in Fig. 2. Here a FTIR spectrum of ethane in nitrogen is shown at a cell temperature of 100 °C as was available from the literature [28]. (The increased temperature only sligthly changes the relative intensities of the absorption peaks in comparison to the room-temperature spectrum.) The strongest absorption features are formed by Q sub-branches: The small differences between the rotational B constants in the lower and upper states result in narrow subbranches; the overlap of the lines at atmospheric pressure results in an enhanced intensity and makes them well suited for the quantification of ethane, for example in atmospheric spectra. With the CO overtone laser, the best concidence between laser line and absorption feature of the C_2H_6 spectrum is at the 24P6 laser line (i.e., transition $v' = 26 \rightarrow v'' = 24$, $J' = 5 \rightarrow J'' = 6$) at 3013.62 cm^{-1} [10].

The experiments showed that desired OPO idler wavelengths could be set without complications. For the subsequent sensitivity tests, measurements were performed at the $^rQ_0$ and $^rQ_3$ sub-branches which have comparable intensity (see Fig. 2).

To first demonstrate the gain in detection sensitivity possible with the OPO thanks to its unrestricted tunability, we compared the PA signals at 3013.62 cm^{-1} (the best coincidence between the CO overtone laser and ethane) and

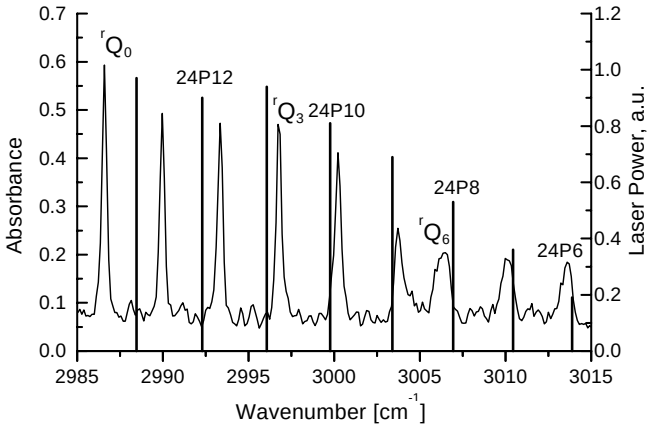

Fig. 2. Portion of the ethane absorption spectrum around 3.000 cm^{-1}. The absorption spectrum was recorded with 83 ppm C_2H_6 in 1 atm N_2 at 100 °C using FTIR with 0.25 cm^{-1} effective resolution [27]. The *vertical lines* indicate the positions (and the relative power available) of the CO overtone laser lines [8] in this region to show the coincidences between laser lines and absorption structures

at the center of the $^rQ_0$ sub-branch (2986.7 cm^{-1}). With the 0.98-ppm ethane mixture the normalized PA signal (= NPAS, per mW idler power) increased from 25 μV/mW to 64 μV/mW, giving an increase in sensitivity by a factor of about 2.5. This makes the strong Q sub-branches well suited for the detection of ethane.

To determine the detection limit for ethane the PA background signal was measured after the PA cell was flushed with N_2 for several hours. Comparing the background of 35 nV/mW with the mentioned ethane signal at the $^rQ_0$ sub-branch yields a sensitivity limit (background equivalent concentration) of about 540 ppt at a power level in the cell of about 40 mW. In Fig. 3 the increase of the PA signal is shown when the gas flow is switched from pure N_2 to the gas mixture.

In order to understand the present sensitivity limitations, several sources have been considered: broadband noise from the laboratory, narrowband noise from the chopper, background caused by coherent wall and window signals, and photoacoustic signals due to parasitic absorptions by impurities in the N_2. These sources were evaluated by successively adding the chopper and infrared beam contributions to the laboratory noise. The microphone signal was measured with a lock-in amplifier at a time constant of 10 s, and the mean value and standard deviation were determined for the in-phase and out-of-phase components, referring to the phase of an ethane signal. The results are given in Table 1. As expected, the laboratory noise contributes mostly randomly to the signal, whereas the chopper gives a signal with a well-defined phase (and no additional noise). When the idler beam is sent through the cell (with about 40 mW inside the PA cell), wall, window, and parasitic gas signals may contribute to the coherent background. Depending on the source and the magnitude of these three contributions, the resulting background signal may have a phase which is different from the phase of an ethane signal. (In an extra-cavity experiment with a CO_2 laser, for example, a window signal phase of $-120°$ was observed [29]). In the present case the superposition of chopper and coherent background signal results in a reduction of the in-phase component of the background.

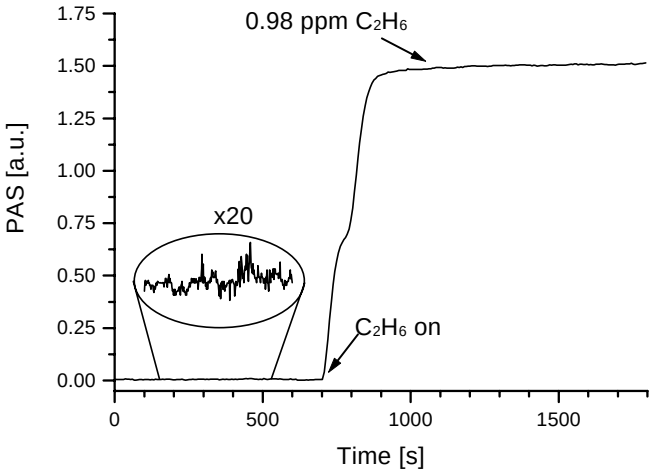

Fig. 3. Comparison of background and ethane signal. Before the measurement the cell was flushed with N_2 for 48 h to ensure minimum background signal. The PA signal was measured at 2996.9 cm^{-1} ($^rQ_3$ sub-branch). To demonstrate the low noise level the background signal has been enlarged 20 times. After about 700 s the gas flow was changed from pure nitrogen to the mixture of 0.98 ppm C_2H_6 in N_2. The reason for the shoulder in the signal slope has not been identified yet

Table 1. Signal contributions with N_2 in the cell. *In-phase* refers to the phase of an ethane signal

	lab noise /μV	lab noise + chopper /μV	lab noise + chopper + idler /μV
in-phase	0.4 ± 2.0	3.3 ± 1.3	0.7 ± 1.2
out-of-phase	0.15 ± 1.2	1.7 ± 1.4	2.1 ± 1.5

The different phase of trace-gas absorption signal and background signal could be observed, for example, when the gas flow through the PA cell was switched between the C_2H_6 mixture and pure nitrogen (see Fig. 4). Here the amplitude and the phase of the PA signal are plotted against time for two consecutive cycles. Removing the ethane from the resonator reduced the gas signal as expected. The increasing

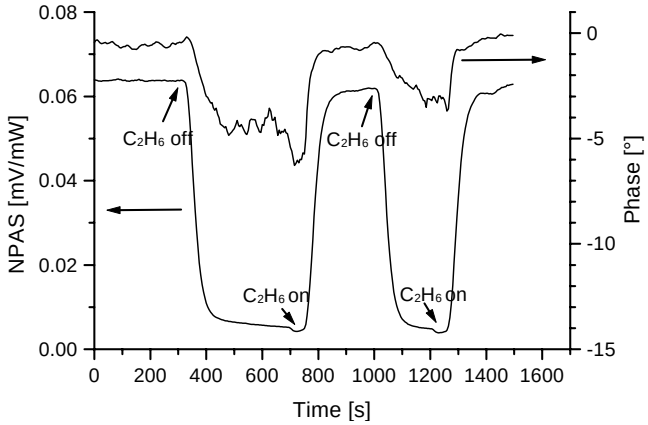

Fig. 4. Phase shift of the normalised photoacoustic signal (NPAS) with changing C_2H_6 concentration in the PA cell. The gas flow is switched between ethane (0.98 ppm in N_2) and pure nitrogen (99.999%) as indicated. Since the gas and the background signal have a different phase relative to the incident infrared beam, the resulting superposition signal changes its phase when the contribution from the gas signal is reduced

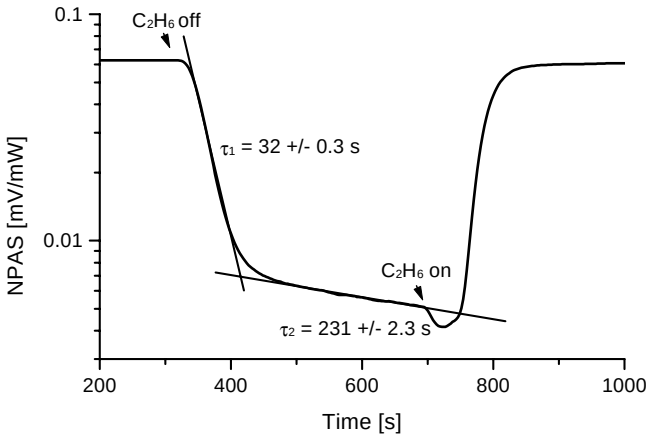

Fig. 5. Decay of the normalised photoacoustic signal (NPAS) with removal of the C_2H_6 from the resonator. A first time constant ($\tau_1 = 32$ s) describes the gas exchange in the resonator (volume 14 cm^3, flow 33 cm^3/min). The second, much slower decay ($\tau_2 = 231$ s) is due to back-diffusion of C_2H_6 from the much larger buffer volumes

influence of the background, on the other hand, was indicated by a small, but significant, change in the PA phase, although the gas component still dominated the amplitude of the signal.

As a final point, the cell loading time response was studied. As can be seen from Fig. 4 the exchange of the gas in the resonator takes place very quickly. The PA signal shows a decay with a time constant of about 30 s – this compares very well with the gas exchange rate at a flow of 2 l/h (33 cm^3/min) and a resonator volume of about 14 cm^3. A logarithmic plot (Fig. 5) reveals, however, that this first decay goes over in a second one with a much higher time constant of about 230 s: While the gas flow exchanges the gas in the resonator very rapidly, the much larger buffer volumes are refilled more slowly. Thus as soon as the bulk amount of C_2H_6 mixture is removed from the resonator back diffusion of C_2H_6 from the buffers into the resonator can be observed resulting in a higher time constant. This is, however, an effect with small practical impact; it becomes obvious only when a sudden switch to low or zero concentrations occurs after a long period of high trace-gas concentrations which are necessary to establish a high stationary concentration in the buffers.

3 Discussion

With the present combination of OPO and photoacoustic cell a detection limit for ethane (C_2H_6) of 0.54 ppb was achieved at an idler power of about 40 mW and with a lock-in time constant of 10 s. This is a very good result compared to the best data for the CO overtone laser. There a background equivalent ethane concentration of about 0.14 ppb was reached with an intracavity power of more than 1 watt [10]. A major contribution to this impressive result comes from the more than twofold gain in the photoacoustic signal when the best overtone coincidence (laser line 24P6) and the strongest absorption feature of ethane (due to the $^rQ_0$ sub-branch) are compared. These data compare well with the FTIR literature data presented in Fig. 2.

Due to the lower power of the OPO in comparison with the CO overtone laser (40 mW vs $>$ 1 W) the broadband noise shows a stronger influence on the detection limit in the present experiment than in the case of the CO overtone

laser. Thus, for measurements in the low-ppb range a time constant of 10 s is at present necessary to suppress the incoherent background noise below the level of the coherent contributions (chopper and photoacoustic background). The CO overtone laser experiments showed a different situation: because of the high laser power levels the detection limit is given by coherent photoacoustic background signals which scale with the laser power. A time constant of 300 ms is thus sufficient to suppress the incoherent noise level below the coherent one.

At higher trace gas concentrations, however, when laboratory noise becomes insignificant in comparison with the photoacoustic signal, the very good amplitude stability of the OPO yielded photoacoustic signals with a very low noise level and thus allowed the changes in gas concentration in the cell to be followed with high accuracy. Switching between the C_2H_6 mixture and pure N_2 removes the bulk gas from the resonator very rapidly, as can be expected from the gas flow rate and the volume to be exchanged. This first decay is followed by a second much slower one due to the time which is necessary to remove the C_2H_6 from the buffers.

In further OPO experiments improved acoustic damping and shielding of the cell will be necessary in order to suppress the incoherent noise and to reduce the coherent chopper background. These measures, together with an increased OPO power and an optimized PA cell will allow a reduction of the measurement time constant and a further improvement of the detection limit.

4 Conclusion

Experiments on trace gas detection using a cw single-frequency broadly tunable OPO are presented. The new system offers continuously tunable radiation with high frequency and power stability at the 100-mW power level in the 2.3–4-μm range. The combination of this new radiation source with a sophisticated photoacoustic detection system results in an ethane detection sensitivity below 1 ppb, which is already close to the best values achieved with conventional LN_2-cooled CO overtone lasers and intracavity configuration. The free wavelength selection will result in improved sensitivity especially for those molecules where the fixed frequencies of the gas lasers offered weak coincidences with the absorption spectrum, as it is the case with methane [30].

The new, compact system opens a great perspective for the development of small mobile trace gas detection systems which can be applied in environmental monitoring as well as in process control (chemistry or biology) where high time resolution and small sample volume are important requirements. Future work will be directed to PA measurements at reduced pressure to allow the simultaneous, selective detection of different species. An essential step for the application of OPO systems for trace gas detection will be the development of mechanisms for the fast wavelength change of the OPO which is at present limited by the necessary temperature changes.

Acknowledgements. This work was supported financially by the German Ministry for Education, Science, Research and Technology, BMBF, under contracts 13N6604 and 13N7025, the Deutsche Forschungsgemeinschaft (DFG), the Optik-Zentrum Konstanz, and the Kurt Lion Foundation.

Klaus Schneider died on March 30, 1998, following a tragic mountaineering accident. He was an excellent scientist, colleague, and friend. His enthusiasm and ideas will remain with us.

Note added

PA detection of methane has been studied by using a setup similar to the one described above. A detection limit of about 300 ppt was achieved, measuring on the absorption peak located at 3067.28 cm^{-1}.

References

1. A. Mandelis, P. Hess (Eds.): *Progress in Photothermal and Photoacoustic Science and Technology*, Volume III: Life and Earth Sciences (SPIE Press 1997)
2. F. Harren, J. Reuss: Spectroscopy, Photoacoustic, In *Encyclopedia of Applied Physics* (VCH, Weinheim 1997) pp. 413–435
3. M.W. Sigrist: Air Monitoring by laser photoacoustic spectroscopy, In *Air Monitoring by Spectroscopic Techniques*, ed. by M.W. Sigrist Chemical Analysis, Vol. 127 (Wiley 1994) pp. 163–238
4. L.B. Kreuzer: J. Appl. Phys. **42**, 2934 (1971)
5. F.J.M. Harren, F.G.C. Bijnen, J. Reuss, L.A.C.J. Voesenek, C.W.P.M. Blom: Appl. Phys. B **50**, 137 (1990)
6. T. Fink, S. Büscher, R. Gäbler, Q. Yu, A. Dax, W. Urban: Rev. Sci. Instrum. **67**, 4000 (1996)
7. S. Bernegger, M.W. Sigrist: Infrared Phys. **30**, 375 (1990)
8. E. Bachem, A. Dax, T. Fink, A. Weidenfeller, M. Schneider, W. Urban: Appl. Phys. B **57**, 185 (1993)
9. S. Büscher, T. Fink, A. Dax, Q. Yu, W. Urban: Photoacoustic Spectroscopy of trace gases expanded to the wavelength of the CO-overtone laser, In: *Optical methods in biomedical and environmental sciences*, ed. by O. Ohzu, S. Komatsu, (Elsevier Science, Amsterdam 1994) pp. 365–368
10. A.A.E. Martis, S. Büscher, F. Kühnemann, W. Urban: Instrum. Sci. Technol. **26**, 177 (1998)
11. T.W. Kimmerer, T.T. Kozlowski: Plant Physiol. **69**, 840 (1982)
12. L. Petruzzelli, F. Harren, C. Perrone, J. Reuss: J. Plant Physiol. **145**, 83 (1995)
13. B. Beßler, S. Schmitgen, F. Kühnemann, R. Gäbler, W. Urban: Planta **205**, 140 (1998)
14. W.C. Eckhoff, R.S. Putnam, S. Wang, R.F. Curl, F.K. Tittel: Appl. Phys. B **63**, 437 (1996)
15. K.P. Petrov, S. Waltman, E.J. Dlugokencky, M. Arborem, M.M. Fejer, F.K. Tittel, L.W. Hollberg: Appl. Phys. B **64**, 567 (1997)
16. M. Feher, P.A. Martin, A. Rohrbacher, A.M. Soliva, J.P. Maier: Appl. Opt. **32**, 2028 (1993)
17. M.J. Johnson, J.G. Haub, B.J. Orr: Opt. Lett. **20**, 1277 (1995)
18. A. Bohren, M.W. Sigrist: Infrared Phys. Technol. **38**, 423 (1997)
19. Ch. Brand, A. Winkler, P. Hess, András Miklós, Zoltán Bozóki, Janós Sneider: Appl. Opt. **34**, 3257 (1995)
20. G.M. Gibson, M.H. Dunn, M.J. Padgett: Opt. Lett. **23**, 40 (1998)
21. R. Al-Tahtamouni, K. Bencheikh, R. Storz, K. Schneider, M. Lang, J. Mlynek, S. Schiller: Appl. Phys. B **66**, 733 (1998)
22. S.T. Yang, R.C. Eckardt, R.L. Byer: J. Opt. Soc. Am. B **10**, 1684 (1993)
23. G. Robertson, M.J. Padgett, M.H. Dunn: Opt. Lett. **21**, 1735 (1994)
24. K. Schneider, S. Schiller: Appl. Phys. B **65**, 775 (1997)
25. K. Schneider, P. Kramper, S. Schiller, J. Mlynek: Opt. Lett. **22**, 1293 (1997)
26. R.L. Myers, R.C. Eckardt, M.M. Fejer, R.L. Byer, W.R. Bosenberg, J.W. Pierce: J. Opt. Soc. Am. B **12**, 2102 (1995)
27. W.R. Bosenberg, A. Drobshoff, J.I. Alexander, L.E. Myers, R.L. Byer: Opt. Lett. **21**, 713 (1996)
28. T.G. Geyer, G.M. Plummer, T.A. Dunder: FTIR Technology Development – Draft Report Entropy Environmetalists, Inc., EPA Contract 68D90055 Work Assignment 2.107, September 1992
29. A. Popp: Diploma thesis, Institute of Applied Physics, University of Bonn 1998
30. St. Büscher: private communication